

THE INTERDEPENDENCE OF PARAMETERS FOR TeV LINEAR COLLIDERS\*

R. B. PALMER

Stanford Linear Accelerator Center,  
 Stanford University, Stanford, California 94305  
 and

Brookhaven National Laboratory, Upton, New York 11973

	Page
1. Damping Ring . . . . .	2
1.1 Emittance . . . . .	2
1.2 Other Requirements . . . . .	4
2. Acceleration . . . . .	5
2.1 Acceleration Cavity . . . . .	5
2.2 Focussing in the Linac . . . . .	7
3. Emittance Preservation . . . . .	7
3.1 Transverse Wake Fields . . . . .	7
3.2 Landau Damping . . . . .	8
3.3 Tolerance Problems . . . . .	9
3.4 Longitudinal Wakes . . . . .	10
4. Final Focus . . . . .	13
5. Interaction Point . . . . .	15
5.1 Luminosity . . . . .	15
5.2 Disruption Angles . . . . .	17
5.3 Beamstrahlung . . . . .	18
6. Round Versus Flat Beams . . . . .	19
7. Parameter Choices . . . . .	21
7.1 Introduction . . . . .	21
7.2 Accelerating Gradient . . . . .	22
7.3 RF Structure Group Velocity . . . . .	23
7.4 Fill Time . . . . .	24
7.5 Damping Ring Impedance $Z/n$ . . . . .	24
7.6 Emittance Ratio $\epsilon_x/\epsilon_y$ . . . . .	25
7.7 Final Focus Pole Tip Field . . . . .	25
7.8 Crossing Angle . . . . .	26
7.9 Particles Per Bunch $N$ . . . . .	26
7.10 Bunch Length $\sigma_x$ . . . . .	28
7.11 Linac Focusing . . . . .	29
7.12 Focus Asymmetry $\beta_x^*/\beta_y^*$ . . . . .	30
7.13 Wall Power . . . . .	31
8. Choice of Wavelength . . . . .	31
8.1 Introduction . . . . .	31
8.2 Luminosity and Beamstrahlung . . . . .	32
8.3 Final Focus Criteria . . . . .	33
8.4 Tolerances . . . . .	33
8.5 Damping Ring Criteria . . . . .	34
8.6 RF Power Source Cost . . . . .	35
8.7 Wavelength Conclusion . . . . .	37
9. Conclusions . . . . .	37
9.1 Warnings . . . . .	37
9.2 Encouragement . . . . .	38
10. Final Remarks . . . . .	38
References . . . . .	39
Appendix I. Parameters Independent of Wavelength . . . . .	40
Appendix II. Parameters Dependent of Wavelength . . . . .	41

\*Work supported by the Department of Energy, contracts DE-AC03-76SF00515 (SLAC) and DE-AC02-76C0016 (BNL).

Presented at the Workshop on New Developments in Particle Accelerator Techniques,  
 Orsay, France, June 29-July 4, 1987

and  
 Invited talk presented at the ICFA Workshop on Low Emittance Beams,  
 Upton, Long Island, New York, March 20-25, 1987

## ABSTRACT

Burt Richter, at SLAC, has called for a design of a 0.5 + 0.5 TeV  $e^+e^-$  collider with a luminosity of at least  $10^{33} \text{ cm}^{-2} \text{ sec}^{-1}$ . In order to find whether such a machine is possible, I have collected here approximate formulae for many of the relations governing the design of a linear collider. It must be emphasized that these are often only approximate relations whose accuracy is not expected to be better than about 10%, and in some cases may be worse. Units throughout will be meter-kilogram-second (mks) unless otherwise stated. Given these relations, their interdependence is studied and parameter choices made. A self-consistent solution is found that meets Richter's specification and does not involve any exotic technologies.

### 1. DAMPING RING

#### 1.1 Emittance

It is assumed that electrons and positrons are obtained from damping rings, and that these are of the continuous wiggler type [1,2]. It is assumed that the phase advances per cell are sufficiently small and that straight sections are sufficiently short so that a smooth approximation ( $\beta \approx \text{constant}$ ) can be used. All bending magnets in the ring consist of at least one inward bend and one outward, so that the average bending field  $\langle B_d \rangle$  is less than the local fields  $B_d$  in the magnets. I define

$$\begin{aligned}\langle B_d \rangle &= \alpha_1 B_d \\ F_m &= \text{fraction of ring filled by dipoles} \\ \zeta &= \text{vertical/horizontal emittance due to mixing}\end{aligned}$$

The emittances both vertical and horizontal are damped by the emission of synchrotron radiation with a time constant [3]:

$$\tau_{x,y} \approx \frac{8.3}{J_{x,y}} \frac{1}{B_d^2 \gamma F_m} \quad (\text{mks}) \quad , \quad (1)$$

where  $J_x, J_y$  are the partition functions [3], usually  $J_x \approx J_y \approx 1$ .

The horizontal ( $x$ ) emittance does not reduce to zero, however, but to an equilibrium value. At high energies this value is set by the effect of quantum fluctuations:

$$\begin{aligned}q\epsilon_{zn} &\approx \frac{2.2 \times 10^{-10}}{(J_x + \zeta J_y)} \beta_x B_d \frac{\gamma^2}{Q_x^2} \quad , \\ q\epsilon_{yn} &= \zeta q\epsilon_{zn} \quad ,\end{aligned} \quad (2)$$

where  $\zeta$  is a mixing parameter,  $\beta_x$  is the average function ( $\beta_x = R/Q_x$ ), and  $Q_x$  is the tune of the ring.

At lower energies intrabeam scattering sets an equilibrium emittance [4]:

$$\begin{aligned}
 c\epsilon_{zn} &\approx \frac{1.2 \times 10^{-10}}{B_d} \left[ \frac{N}{\epsilon_{zn} \gamma F_m Q \zeta (J_x + \zeta J_y)} \left( \frac{\beta_x}{\beta_y} \right)^{1/2} \right]^{1/2} , \\
 c\epsilon_{yn} &= \zeta c\epsilon_{zn} , \\
 \epsilon_{zn} &= \gamma \frac{dp}{p} \sigma_x .
 \end{aligned} \tag{3}$$

We note from the different  $\gamma$  dependencies that there must be an optimum  $\gamma_0$  for which  $c\epsilon = q\epsilon$  (see Fig. 1).

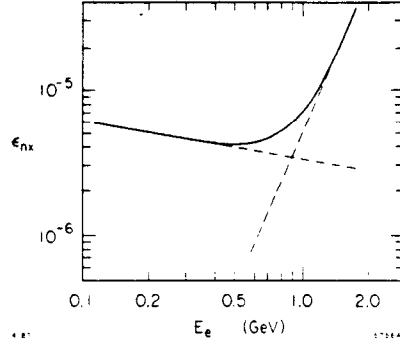


Fig. 1. The normalized emittance of a sample ring, as a function of operating electron energy. As  $E$  is varied the ring is varied to keep the bending field  $B_d$ , the focussing field  $B_q$  and the tune  $Q$  fixed. At low energies the emittance is dominated by intrabeam scattering, at high energies by quantum fluctuations.

$$\gamma_0 \approx 2.1 \times 10^{-7} \left[ \frac{N (B_y/B_x)^{1/2}}{\epsilon_{zn} B_d^{2.5} \zeta (J_x + \zeta J_y)^{1/2} F_m k_1^{1/2}} \right]^{4/9} \left( \frac{1}{\epsilon_{zn}} \right)^{2/3} , \tag{4}$$

where

$$\beta_x = k_1 \gamma^{1/2} \approx k \left( \frac{a\gamma}{B_q F_q} \right)^{1/2} \tag{5}$$

$a$  = quadrupole aperture

$B_q$  = quadrupole pole tip field ( $\approx 1.5$  Tesla)

$F_q$  = fraction of ring full of quads ( $\approx .2$ )

$k_1$  = .14, for a lattice scaled from the SLAC damping ring.

When contributions from both quantum fluctuations and intrabeam scattering are comparable, then the equilibrium emittance is given [4] by

$$\epsilon_{zn}(\text{equilib}) = \frac{1}{2} \left[ q\epsilon_{zn} + (q\epsilon_{zn}^2 + 4c\epsilon_{zn}^2)^{1/2} \right] , \quad (6)$$

thus for  $q\epsilon_{zn} = c\epsilon_{zn}$

$$\epsilon_{zn}(\text{equilib}) \approx 1.6 q\epsilon_{zn} . \quad (7)$$

Actually a minimum equilibrium is obtained at a  $\gamma$  somewhat below that given by Eq. (4) and it is a reasonable approximation to use

$$\epsilon_{zn} \approx 1.4 q\epsilon_{zn} . \quad (8)$$

The wiggler is assumed to consist of a sufficient number of inward and outward bends, so that the contribution to the emittance from the rate of change of dispersion is negligible. This condition requires the maximum wiggler pole length  $\ell_w$  to satisfy

$$\ell_w \ll \ell_w^{\text{max}} = \sqrt{\frac{8}{F_m}} \frac{\beta_z \rho}{R} , \quad (9)$$

where  $\rho$  is the bending radius in a wiggler and  $R$  is the average machine radius. In these examples I assume  $\ell_w = 1/3(\ell_w^{\text{max}})$  and the contribution to the equilibrium emittance is then less than 1/9.

## 1.2 Other Requirements

The impedance requirement for stability is taken to be:

$$\frac{Z}{n} \leq \frac{(2\pi)^{3/2} \sigma_x (E/e) \alpha \sigma_p^2}{c e N} , \quad (10)$$

where

$$n = \frac{R}{\sigma_x} , \quad (11)$$

$$\alpha \approx \left( \frac{\beta_z}{R} \right)^2 = \frac{1}{Q^2} . \quad (12)$$

Note that the approximation for the momentum compaction  $\alpha$  also requires condition [Eq. (9)].

Other relations are:

$$\sigma_p = \frac{\Delta p}{p} \approx \frac{2}{J_x} 1.1 \times 10^{-5} (\gamma B)^{1/2} , \quad (13)$$

$$\text{Dispersion } \eta \approx \frac{\beta_z^2}{R} , \quad (14)$$

$$\text{Sextupole length } F_s \approx F_q \frac{a}{4\eta} , \quad (15)$$

$$\text{acceptance } \hat{\epsilon}_{zn} \approx 6 \times 10^{-4} \gamma R \frac{Q_y}{Q_z^4} , \quad (16)$$

$$\text{RF Volts/turn } U \approx 3.2 \times 10^6 \frac{\gamma}{h} \left( \frac{R}{Q_z} \frac{\sigma_p}{\sigma_x} \right)^2 , \quad (17)$$

where  $h$  is the harmonic number of the RF,

$$\text{energy loss/turn } V = 5.78 \times 10^{-9} \frac{\gamma^4}{\alpha^2 R F_m} . \quad (18)$$

## 2. ACCELERATION

### 2.1 Acceleration Cavity

I assume that acceleration takes place in a  $2\pi/3$  disk-loaded-structure as used in the SLAC linac, but following Z. D. Farkas [5], I allow the group velocity to depart from that of the SLAC structure. Since the group velocity is a function of the iris aperture divided by the wavelength, we can choose these parameters separately and use an approximate fit to Farkas' calculation using the program TWAP [5] (see Fig. 2a):

$$\beta_g = \frac{v_g}{c} \approx \exp \left\{ 3.1 - 2.4 \left( \frac{\lambda}{a} \right)^{1/2} - .9 \left( \frac{a}{\lambda} \right) \right\} \quad (19)$$

The normalized corrected elastance is given approximately by (see Fig. 2b)

$$s_{at} \approx 5.7 \times 10^{10} \beta_g^4 \quad (\text{Vmc}^{-1}) \quad (20)$$

This normalized and corrected elastance is related to the unnormalized elastance by

$$s_{at} = s_t a^2 \quad , \quad (21)$$

where  $s_t$  is defined by

$$s_t = \frac{\mathcal{E}_a^2}{w_f} \quad , \quad (22)$$

$\mathcal{E}_a$  is the average accelerating field in a section and  $w_f$  is the energy, assuming no losses, needed to generate that acceleration. This energy is not the same as that required ( $w$ ) to fully fill the section because since the particle and fields are moving down the section at finite velocity, the length of the required field pulse is less than that of the section. Thus

$$w_f = \frac{w}{(1 - \beta_g)} \quad , \quad (23)$$

and

$$s_t = \frac{s}{(1 - \beta_g)} \quad , \quad (24)$$

where the uncorrected elastance, as defined by D. Farkas is

$$s = \frac{\mathcal{E}_a^2}{w} \quad . \quad (25)$$

Note also that  $s$  is related to the loss parameter defined by P. Wilson: [6]

$$k_0 = \frac{s}{4} \quad . \quad (26)$$

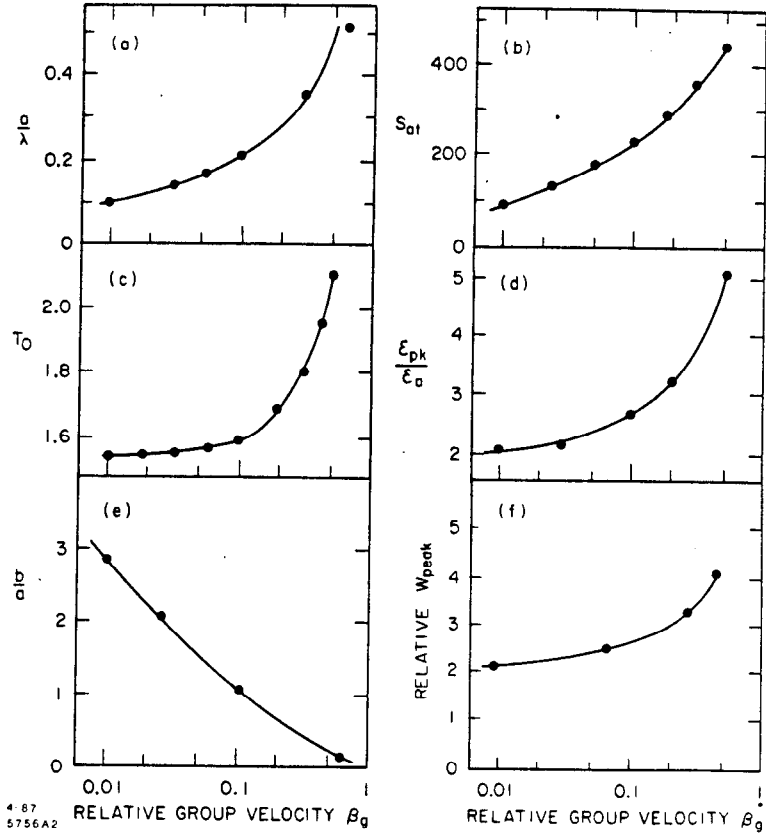


Fig. 2. Parameters of a SLAC-like accelerating cavity as a function of the group velocity  $v_g/c = \beta_g$ . (a) the iris radius  $a$  divided by wavelength  $\lambda$ ; (b) the normalized corrected elastance  $s_{01}$ ; (c) the attenuation time constant  $T_0$  in  $\mu\text{sec}$ , for  $\lambda = 10.5$  cm; (d) the peak RF field in the cavity  $\mathcal{E}_{pk}$  divided by the average accelerating field  $\mathcal{E}_a$ ; (e) the outer cavity radius  $b$  divided by the iris radius  $a$ ; (f) the relative peak rf power. In each case the line is obtained from Z. D. Farkas [5] and the dots are for the approximation used here.

When losses are included, the energy needed is increased. If the attenuation time of the RF pulse, passing down the section, is defined as  $T_0$ , then for a section of length  $L$  the energy required for the same average acceleration will be:

$$w_{RF} = \frac{\omega_f}{\eta_\rho} = \omega_f \frac{\tau^2}{(1 - e^{-\tau})^2}, \quad (27a)$$

where  $\eta_\rho$  is the section efficiency, and

$$\tau = \frac{L}{T_0 v_g} = \frac{T}{T_0}. \quad (27b)$$

This is for a uniform structure (i.e.,  $\mathcal{E}_a$  falling off along its length). Note that as  $\tau \rightarrow 0$ ,  $w_{RF} \rightarrow \omega_f$  but the peak power per unit length goes to  $\infty$ .

The attenuation time  $T_0$  is given approximately by (see Fig. 2c):

$$T_0 \approx 42 \times 10^{-6} (1 + 1.29 \beta_g^{1.5}) \lambda^{1.5} , \quad (28)$$

also (see Figs. 2d and e):

$$\frac{\mathcal{E}_{pk}}{\mathcal{E}_a} \approx 2 + 6.0 \beta_g , \quad (29)$$

$$\frac{b}{a} \approx 1.04 + 0.29 \ln \left( \frac{1}{\beta_g} \right) + .068 \left[ \ln \left( \frac{1}{\beta_g} \right) \right]^2 , \quad (30)$$

where  $\mathcal{E}_{pk}$  is the maximum field within the structure and  $b$  is the inside radius of the cavity. In all cases the length of a cell is assumed to be  $\lambda/3$ .

All of the above approximate relations were obtained by fitting curves shown in Farkas and Wilson's paper [5].

## 2.2 Focussing in the Linac

Assuming a symmetric FODO structure, the average strength of the focussing is given by

$$\langle \beta_x \rangle = \left( \frac{\sin \mu}{\mu^2} \frac{E}{c} \frac{2a_q}{B_q F_q} \right)^{1/2} , \quad (31)$$

where  $\mu$  is the phase advance per half cell (taken as  $45^\circ$ ),  $B_q$  is the pole tip field (taken as 1.5 Tesla),  $F_q$  is the fraction of linear length devoted to quadrupoles, and  $a_q$ , the aperture of the quad, is taken to be  $1.2 \times a_{av}$ . Normally,  $a_{av}$  is the iris radius, but if the iris is elliptical with radii  $a$  and  $b$ :

$$a_{av} = \frac{1}{\left( \frac{2}{a^2} + \frac{2}{b^2} \right)^{1/2}} , \quad (32)$$

which is the radial distance at  $45^\circ$ .

## 3. EMITTANCE PRESERVATION

### 3.1 Transverse Wake Fields

The transverse wake field  $W_t$  depends on the geometry of the cavities. As a function of the length  $z$  along the bunch, the wakefield is observed [6] to have an initial linear rise:

$$\text{for } z \ll a: \quad {}_1W_t(z) \approx 6.64 \times 10^{10} \frac{z}{a^{3.5} \lambda^{1.5}} , \quad (33)$$

and a maximum of

$$\text{at } z \approx a: \quad {}_2W_t(z) \approx 3.28 \times 10^{10} \frac{1}{a^{2.2} \lambda^{1.8}} . \quad (34)$$

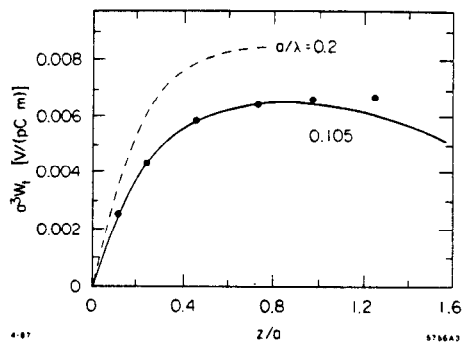


Fig. 3. The scale invariant transverse wakefield ( $a^3 W_t$ ) as a function of the distance  $z$  divided by the iris radius  $a$  for (a)  $a/\lambda = .105$  (as for SLAC), and (b)  $a/\lambda = .2$

For values of  $W_t$  at  $z/a < 1$ , a reasonable fit to the form of  $W$  [at least for the SLAC geometry (see Fig. 3)] is obtained if we take:

$$W_t = \frac{1}{\left(\frac{1}{1W_t^2} + \frac{1}{2W_t^2}\right)^{1/2}} \quad (35)$$

The approximation is seen to be reasonable in the region  $z < a$ .

In the case of an elliptical iris with dimensions  $a$  and  $b$ , I assume the same form as given above with the substitution of  $a$  or  $b$  according to whether we are calculating  $W_t$  in the  $x$  or  $y$  directions.

### 3.2 Landau Damping

I assume that transverse wake effects are effectively controlled by *Landau damping* [7], providing an energy spread  $\Delta E$  is maintained between the front and back of the bunch where, in the two bunch approximation:

$$2E\sigma_p \approx \Delta E \approx \frac{e}{4} N W_t(2\sigma_x) \beta^2 \quad (36)$$

where  $N$  is the number of particles per bunch,  $\beta$  the focussing strength in the linac and  $W_t(z)$  is the wake field potential. Both  $W_t$  and  $\beta$  are allowed to be different in the vertical and horizontal directions, but chosen so as to give the same required  $\Delta E$ . For tolerance reasons that will appear below, I assume

$$\beta_{x,y} \propto \ell^{1/3} \quad (37)$$

thus

$$\sigma_p \propto \ell^{-1/3} \quad (38)$$

where  $\ell$  is the length along the linac. If not specified,  $\beta$  and  $\Delta E$  are given for the end of the linac — i.e., at full energy.

I will assume that the momentum spread  $dp/p = \sigma_p$  required for Landau damping is maintained until the end of all acceleration, but then removed prior to the final focus by an acceleration section of length  $\ell_c$  operating at a phase advance of  $90^\circ$ . The length required is

$$\ell_c = \frac{\sigma_p p \lambda}{2\pi \mathcal{E}_a \sigma_z} \quad (39)$$

where  $p$  is the final momentum,  $\lambda$  the wavelength,  $\mathcal{E}_a$  the accelerating gradient and  $\sigma_z$  the rms bunch length.

### 3.3 Tolerance Problems

A severe tolerance problem comes from the effects of the finite momentum spread and strong focussing needed to Landau damp the transverse wake field effects. From R. Ruth I take the required rms alignment for phase advance per cell  $\psi$ , to be [8]:

$$\langle dy \rangle = \sigma_y \frac{2}{\psi \sigma_p} \sqrt{\frac{2}{N_q}} \quad (40)$$

where

$$\sigma_y = \sqrt{\frac{\beta(\ell) \varepsilon_y}{\gamma(\ell)}} \quad (41)$$

and  $N_q$ , the number of quadrupoles, is

$$N_q = \int_0^L \frac{2d\ell}{\beta(\ell)\psi} \quad (42)$$

and from Eq. (36) we have

$$\sigma_p \propto \frac{\beta(\ell)^2}{\gamma} \quad (43a)$$

so

$$\langle dy \rangle \propto \frac{\gamma^{1/2}}{\beta(\ell)^{3/2}} \quad (43b)$$

We see that unless the  $\beta$  is reduced at lower  $\gamma$ , the tolerances get tighter at lower  $\gamma$ . However, the quadrupole tip fields needed to obtain a given  $\beta$  also fall with  $\gamma$  [from Eq. (31)].

$$\beta(\ell) \propto \left( \frac{\gamma a}{B_q} \right)^{1/2} \quad (44a)$$

so it is not difficult to assume, for instance:

$$\beta(\ell) \propto \gamma^{1/3} \propto \ell^{1/3} \quad (44b)$$

which gives

$$\text{Tolerances: } \langle dy \rangle = \text{constant} \quad ,$$

$$\begin{aligned}
\text{Landau:} \quad \sigma_p &\propto \gamma^{-1/3} , \\
\text{Focus B:} \quad B_q &\propto \gamma^{1/3} .
\end{aligned}
\tag{44c}$$

Then from Eq. (42),

$$\begin{aligned}
N_q &= 1.5 \left[ \frac{2L}{\beta(\max)\psi} \right] , \\
\langle dy \rangle &\approx 1.63 \frac{\beta(\max)}{\sigma_p(\max)} \left( \frac{\epsilon_n}{\gamma L \psi} \right)^{1/2} .
\end{aligned}
\tag{45}$$

This tolerance concerns the alignment and steering precision within the linac. If all components were truly aligned to this accuracy, it would meet the requirement, but it can also be met by an appropriate combination of alignment and corrective steering that is somewhat less severe.

Another interesting quantity is the change in phase advance  $\Delta\phi$  over the momentum spread integrated along the full accelerator. If this quantity is small compared to 1, then the dispersive errors due to misalignment appear at the end as a single lateral dispersion that could in principle be measured and corrected.

$$\begin{aligned}
\Delta\phi &= \int_0^L \sigma_p(\ell) \frac{d\ell}{\beta(\ell)} , \\
&= \frac{1.5 L \sigma_p(\max E)}{\beta(\max E)} .
\end{aligned}
\tag{46}$$

A tolerance of a different kind concerns the allowable random movement of components from pulse to pulse. Fixed misalignments can often be corrected, but random movements cannot. The most severe restriction is on random motion of the linac focusing quadrupoles. For  $90^\circ$  phase advance per cell:

$$\langle dx \rangle, \langle dy \rangle, \approx \frac{2}{5} \frac{\sigma_{x,y}}{\sqrt{N_q}} ,
\tag{47}$$

where  $N_q$  is the number of quadrupoles from Eq. (42) or (45).

### 3.4 Longitudinal Wakes

The *Longitudinal wake* for very short bunches tends towards a constant that is dependent only [9] on the iris aperture 'a':

$$z \ll a : \quad {}_1W = 1.78 \times 10^{10} \frac{1}{a^2} .
\tag{48}$$

For the elliptical case, I assume

$$z \ll a : \quad {}_1W = 1.78 \times 10^{10} \left( \frac{.5}{a_x^2} + \frac{.5}{a_y^2} \right) .
\tag{49}$$

For bunches of length of the order of 'a' one finds [9]:

$$z \approx a : {}_2W = 1.25 \times 10^{10} \left(\frac{1}{z}\right)^{1/2} \frac{1}{a} \left(\frac{1}{\lambda}\right)^{1/2} \quad (50)$$

And for the elliptical case I assume

$$z \approx a : {}_2W = 1.25 \times 10^{10} \left(\frac{1}{z}\right)^{1/2} \left(\frac{.5}{a_x} + \frac{.5}{a_y}\right) \left(\frac{1}{\lambda}\right)^{1/2} \quad (51)$$

For intermediate values of  $z$ , a reasonable fit to the SLAC case is obtained (see Fig. 4):

$$W_L(z) = \left( \frac{1}{\frac{1}{{}_1W^3} + \frac{1}{{}_2W^3}} \right)^{1/3} \quad (52)$$

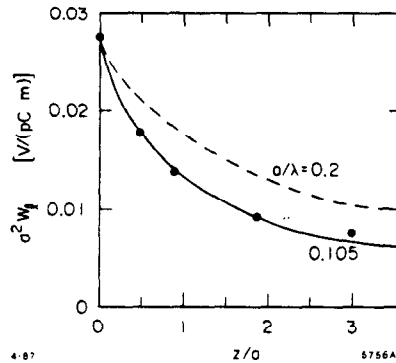


Fig. 4. The scale invariant longitudinal wakefield ( $a^2 W_L$ ) as a function of the length  $z$  divided by the iris radius  $a$  for (a)  $a/\lambda = .105$  (as for SLAC), and (b)  $a/\lambda = .2$

To properly obtain the momentum spread produced in a bunch by the longitudinal wake, one should perform integrations of the wake potentials over the charge distribution of the bunch [6]. The effects are relatively complex:

- 1) There is an average energy loss of the bunch (zeroth order).
- 2) There is a greater loss to the back of the bunch compared with the front (first order).
- 3) If the bunch is long there is a significant second order term with the rate of change of momentum falling at the back.
- 4) There is a significant third order term that arises if the bunch is Gaussian rather than uniform in current density.

Since all these are significant, the minimum number of sub-bunches that we can use to approximate the whole is four. I use four equal bunches: two at  $\pm 1.4\sigma_z$  and two at  $\pm .2\sigma_z$ . (These give correct  $\sigma_z$  and  $\langle|z|\rangle$ ). The energy losses of the four bunches are then:

$$\begin{aligned}
V_1 &= \frac{N e}{4 \mathcal{E}_a} \{W(0)\} \quad , \\
V_2 &= \frac{N e}{4 \mathcal{E}_a} \{W(0) + W(1.2 \sigma_x)\} \quad , \\
V_3 &= \frac{N e}{4 \mathcal{E}_a} \{W(0) + W(.4 \sigma_x) + W(1.6 \sigma_x)\} \quad , \\
V_4 &= \frac{N e}{4 \mathcal{E}_a} \{W(0) + W(1.2 \sigma_x) + W(1.6 \sigma_x) + W(2.8 \sigma_x)\} \quad .
\end{aligned}
\tag{53}$$

These values are compared with a full integration in Fig. 5.

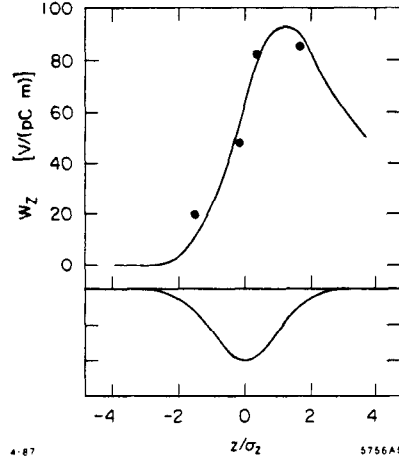


Fig. 5. The longitudinal wakefield generated momentum spread generated in a Gaussian bunch passing through a SLAC-like structure. The smooth line is a calculation by P. Wilson [6]. The dots represent the results of the four-bunch approximation used here. These points have been normalized to the P. Wilson calculation.

The average slope gives a  $\Delta p$  at  $1\sigma$  of

$$1\sigma_p = \frac{.2(V_3 - V_2) + 1.4(V_4 - V_1)}{4} \quad .
\tag{54}$$

The half spread due to the second order effect is:

$$2\sigma_p = \frac{(V_3 + V_2) - (V_4 + V_1)}{4} \quad ,
\tag{55}$$

and the half spread from third order:

$$3\sigma_p = \frac{.87(V_3 - V_2) + .13(V_4 - V_1)}{4} \quad .
\tag{56}$$

The first and second of these effects can in principle be cancelled by the RF. The first order effect

being cancelled by a phase shift in the RF given by

$$\tan \phi_{\text{cor}} = \frac{1}{2\pi} 1\sigma_p \frac{\lambda}{\sigma_x} . \quad (57)$$

However, some momentum spread is required for Landau damping so that the phase required at the end is, instead, given by

$$\tan \phi_{\text{cor}} = \frac{1}{2\pi} (1\sigma_p - \sigma_p(\text{Landau})) \frac{\lambda}{\sigma_x} . \quad (58)$$

The net second order momentum spread, including the RF is

$$2\sigma_p(\text{total}) = 2\sigma_p - \frac{1}{2} \left( \frac{2\pi\sigma_x}{\lambda} \right)^2 . \quad (59)$$

For the purposes of designing the final focus system, I assume that the first order term is fully cancelled by the RF and use:

$$\sigma_p(\text{focus}) = \left\{ 2\sigma_p(\text{total})^2 + 3\sigma_{p3}^2 + \epsilon\sigma_p^2 \right\} , \quad (60a)$$

where

$$\epsilon\sigma_p = \frac{\epsilon_{zn}}{\gamma\sigma_x} , \quad (60b)$$

which is the contribution to the momentum spread from the finite longitudinal emittance in the damping ring.

#### 4. FINAL FOCUS

The parameters for the final focus are obtained by scaling one of two designs provided by K. Brown [10]. In both cases the minimum  $\beta_0^*$  is calculated for a given momentum spread assuming no chromatic correction. The value of  $\beta^*$  that can be obtained with chromatic correction is less than  $\beta_0^*$  by a factor  $S$

$$\beta^* \geq \frac{\beta_0^*}{S} . \quad (61a)$$

$S$ , in a design similar to that in the SLC is expected [10] to scale:

$$S = \frac{S_0}{\sigma_p} \approx \frac{0.04}{\sigma_p} . \quad (61b)$$

This relation gives a factor of eight for  $\sigma_p = \pm 5\%$  as is obtained for the SLC.

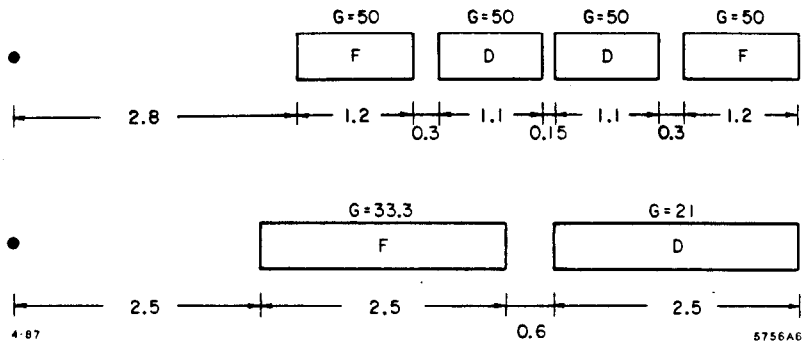


Fig. 6. Final focus lens designs used (a) for solutions requiring a round focal spot and (b) for solutions requiring a flat beam.

The two designs used are shown in Fig. 6. The triplet is used for the symmetric case and the doublet for all asymmetric cases. The scaling involves the modification of all length dimensions by one factor and all transverse dimensions by another. We define scale factors  $f^*$  and  $a^*$ .  $a^*$  is the aperture in the first quadrupole, and the 'ideal' focal length is  $f^*$ :

$$f^* = \left[ \frac{a^*}{B^*} (B\rho) \right]^{1/2}, \quad (62)$$

$$(B\rho) = \frac{E/e}{c}.$$

$B^*$  is the pole tip field in the first quad,  $E/e$  is the beam energy in electron Volts, and  $c$  is the velocity of light.

For any magnet system we can now express the performance in terms of these scaling parameters,  $a^*$  and  $f^*$ , and of invariant constants ( $T_x$ ,  $T_y$ ,  $A_x$ ,  $A_y$  and  $L$ ). The constants depend on the details of the magnet system considered.

Given  $f^*$  and  $a^*$  for any magnet system scaled from the original design (all longitudinal distances scaled with  $f^*$ , all transverse distances scaled with  $a^*$ , all pole tip fields the same) then we can write

$$\beta_{0x,y}^* = T_{x,y} \cdot 2\sigma_p \cdot f^* \quad (63)$$

$$\hat{\theta}_{x,y} = \frac{a^*}{A_{x,y} f^*} \quad (64)$$

$$\ell_1 = L f^* \quad (65)$$

where  $\ell_1$  is the free space before the first quad,  $\hat{\theta}$  is the maximum angular acceptance,  $\sigma_p$  is the rms  $dp/p$  momentum spread. The definitions are such that for an 'ideal' focussing system that can focus in both directions (such as a lithium or plasma lens)  $T \approx A \approx L \approx 1$ .

Combining Eq. (63) with Eq. (61), one obtains:

$$\beta_{x,y}^* = \frac{(T_{x,y} A_{x,y})}{S_0} \frac{E/c}{B^*} \hat{\theta}_{x,y} \sigma_p^2 \quad (66)$$

Values for  $T_{x,y}$  and  $A_{x,y}$  for the two focus designs given are:

	<u>Triplet</u>	<u>Quadrupole</u>
$T_x$	2.96	7.2
$T_y$	2.96	1.1
$A_x$	4.3	3.6
$A_y$	3.2	2.0
$L$	1.36	1.1
$T_y A_y$	9.47	2.2
$S_0$	0.04	0.04

We note that the product  $T_y A_y$  which determines the  $\beta_y^*$  obtainable is over four times smaller for the quadrupole solution.

The maximum acceptance angle  $\hat{\theta}$  is controlled by the disruption angles or beam size depending on whether the crossing is head-on or at a finite angle. In the head-on case the disruption angles are discussed in the next section and we take

$$\hat{\theta}_{x,y} = S_\theta \hat{\theta}_D(x,y) \quad , \quad (67)$$

where  $S_\theta$  is a safety factor taken to be three. In the finite angle case

$$\hat{\theta}_{x,y} = S_\theta \sqrt{\frac{\epsilon_n}{\beta^* \gamma}} \quad , \quad (68)$$

where  $S_\theta$ , the safety factor, is now taken to be six.

## 5. INTERACTION POINT

### 5.1 Luminosity

When the two bunches collide, the luminosity obtained is

$$L = \frac{N^2 f H_x H_y}{4\pi \sigma_x \sigma_y} \eta_L \quad , \quad (69)$$

where

$$\sigma_{x,y} = \left( \frac{\epsilon_{x,y} \beta_{x,y}^*}{\gamma} \right)^{1/2} \quad , \quad (70)$$

and  $\eta_L$  is an efficiency factor to allow for effects of both a finite angle of crossing and a  $\beta^*$  not very much larger than the bunch length  $\sigma_z$ .

$$\eta_L = \frac{2}{\sigma_x \sqrt{\pi}} \int_0^{\infty} \frac{\exp \left\{ - \left( \frac{z}{\sigma_x} \right)^2 \left[ 1 + \frac{\theta_c}{\theta_d} \left( \frac{1}{1 + (z/\beta_z)^2} \right) \right] \right\}}{1 + (z/\beta_z)^2} dz, \quad (71)$$

where  $\theta_d = \sigma_z/\sigma_x$  is the diagonal angle,  $\theta_c$  is the crossing angle, and  $\beta_z$  is the  $\beta_z^*$  at the final focus.

$H_x$  and  $H_y$  in Eq. (69) are enhancement factors due to the pinch effect. I have assumed here that these enhancements can be factorized and that

$$H_{x,y} = f(D_{x,y}), \quad (72)$$

where  $D_{x,y}$  are disruption parameters defined by

$$D_{x,y} = \frac{\sigma_x}{f_{x,y}}, \quad (73)$$

and  $f_{x,y}$  are the effective focal length of the focussing of one bunch on the other, calculated for the center of Gaussian bunches.

Assuming a beam in which  $\sigma_x \geq \sigma_y$  then [11]

$$D_y \approx \frac{r_e N \sigma_z}{\gamma \sigma_y^2} \cdot \frac{2}{1 + \frac{\sigma_x}{\sigma_y}} \quad (74)$$

For round beams  $D_x = D_y$ , but for flat beams with  $\sigma_x \gg \sigma_y$ ,  $D_x \approx 0$ . In the intermediate region we take [11]

$$D_x \approx \frac{r_e N \sigma_x}{\gamma \sigma_x^2} \cdot \frac{2}{1 + \frac{\sigma_x}{\sigma_y}} \quad (75)$$

The enhancements are given approximately [12] by

$$H_{x,y} = 1 + 1.37 \left( \frac{1}{1 + D_{x,y}^{-5.5}} \right)^{1/2} \quad (76)$$

For round beams the more conventional enhancement factor  $H = H_x H_y = (H_y)^2$ . This, calculated by this approximation, is plotted in Fig. 7 against  $D$  and compared with values given by other simulations [12].

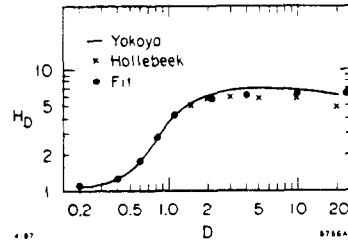


Fig. 7. The luminosity enhancement  $H_D$  for round beams as a function of the disruption parameter  $D$ . The smooth line shows the results of K. Yokoya's calculation [13]; the crosses are Hollebeck's; the dots are the approximation used here.

## 5.2 Disruption Angles

Without pinch, the maximum Disruption angle is given [13] by

$$\hat{\theta}_{x,y} = \frac{2N r_e}{\gamma \sigma_z} \cdot k_{x,y} \quad (77)$$

where for

$$\begin{aligned} \text{(a)} \quad \sigma_x = \sigma_y \quad k &\approx .45 \\ \text{(b)} \quad \sigma_x > \sigma_y \quad \begin{cases} k_x \approx .75 \\ k_y \approx 1.25 \end{cases} \end{aligned} \quad (78)$$

However, the situation is somewhat different in the three cases. For  $\theta_x$  and for  $\theta_y$  in round beams a well-defined maximum angle occurs for particles at a finite impact parameter near  $\sigma$ . But for  $\theta_y$  in flat beams the deflecting field rises to a plateau and the maximum angle occurs only for particles in the extreme tail of the distribution. As a result, the mean value is much less in this case.

With pinch, the round case has been studied by Minten and Yokoya [13] and the disruption is enhanced by a factor  $H_\theta$

$$H_\theta \approx \frac{1}{\left(\frac{1}{1.2 + 50 D^3}\right) + \left(.06 + \frac{D}{3.38}\right)^{1/2}} \quad (79)$$

Figure 8 shows this function together with Minten and Yokoya's simulation.

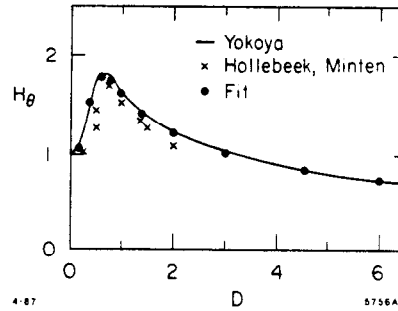


Fig. 8. The enhancement of disruption angles  $H_\theta$  for round beams. The line is Yokoya's calculation; the crosses are Hollebeek and Minten's; and the dots the approximation used.

For flat beams the enhancement of maximum deflection in the vertical ( $y$ ) direction should not occur. This is because the field for a current sheet is not a function of its thickness. However, Yokoya has demonstrated that with a Gaussian bunch, a strong suppression of the average vertical disruption angle takes place for large  $D$  due to the oscillation of a particle in the field instead of a unidirectional deflection. In principle the deflection of the extreme tail of the distribution is still not changed and my program does not include this Yokoya [13] suppression.

In this discussion I have not included quantum fluctuations in the disruption process. There is a finite probability that an electron radiates a hard photon and is then, because it has a low momentum, disrupted by a much larger angle:

$$\theta_D(\text{quantum}) = \theta_D \left( \frac{E_e}{E_e - E_\gamma} \right) \quad (80)$$

The factor  $E_e/(E_e - E_\gamma)$  can be large and the resulting disruption would be a serious problem. In round beams there seems little that can be done about it and larger quads and the resulting weaker focus would have to be employed. But with finite crossing angles one can employ a bending magnet to sweep the low energy disrupted electrons away from the quadrupole (Fig. 9).

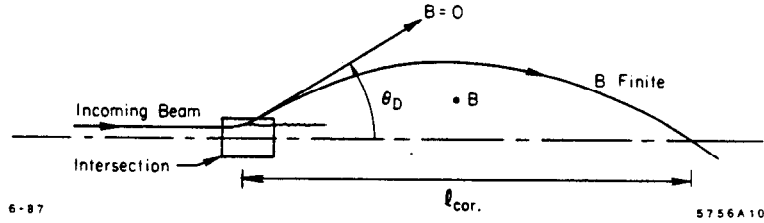


Fig. 9. The use of a sweeping magnet to return disrupted particles to the axis. Such correction will work independent of the beamstrahlung energy loss and resulting enhancement of the disruption angle.

The field length required to return electrons that had the maximum disruption angle  $\theta_D$  is:

$$l_{sweep} = 2 \frac{\theta_D (E/e)}{Bc} \quad (81)$$

where  $E/e$  is the beam energy in electron volts,  $B$  is the correction field and  $c$  the velocity of light.

### 5.3 Beamstrahlung

The beamstrahlung calculations are taken from the work of R. Noble [14]. The fractional loss of energy of one bunch passing through the other is given by

$$\delta = \frac{F_1 r_e^3 N^2 \gamma}{\sigma_x (\sigma_y')^2} \left[ \frac{4}{\left(1 + \frac{\sigma_z'}{\sigma_y'}\right)^2} \right] H_T \quad (82)$$

where  $F_1 \approx .22$ ,  $r_e \approx 2.82 \times 10^{-15}$  m. In this form I have replaced the enhancement factor  $H_D$  that could account for the pinch effect by replacing the unpinned spot sizes ( $\sigma_x$  and  $\sigma_y$ ) by effective 'pinched' values ( $\sigma_x'$  and  $\sigma_y'$ )

$$\begin{aligned} \sigma_x' &= \frac{\sigma_x}{H_x} \quad , \\ \sigma_y' &= \frac{\sigma_y}{H_y} \quad . \end{aligned} \quad (83)$$

In the symmetric case  $H_x H_y = H_D$ . For a flat beam,  $\sigma_x \gg \sigma_y$ :

$$\delta \approx \frac{F_1 r_e^3 N^2 \gamma}{\sigma_x} \frac{4}{(\sigma_x')^2} H_T, \quad (84)$$

and is not a function of  $\sigma_y$ . Note also that in this flat beam case  $H_x$  is usually near to unity (there is little disruption in the wide direction), and thus there is no pinch enhancement of the beamstrahlung.

The parameter  $H_T$  is a correction for quantum effects [14]:

$$H_T \approx \left( \frac{1}{1 + 1.33 \Upsilon^{2/3}} \right)^2, \quad (85)$$

where

$$\Upsilon = \frac{F_2 r_e \lambda_e \gamma N}{\sigma_x \sigma_y'} \cdot \left[ \frac{2}{1 + \frac{\sigma_x'}{\sigma_y'}} \right], \quad (86a)$$

where

$$F_2 \approx .43, \quad r_e \approx 2.82 \times 10^{-15}, \quad \lambda_e \approx 3.86 \times 10^{-13} \text{ m}. \quad (86b)$$

Note again that I have expressed  $\Upsilon$  as a function of the effective spot dimensions  $\sigma_x'$  and  $\sigma_y'$ . And we also note again that for  $\sigma_x' \gg \sigma_y'$ ,  $\Upsilon$  is a function only of  $\sigma_x'$  and that this is *not* significantly enhanced by pinch. This is again a reflection of the fact that the fields in a flat beam are a function of the width of that beam, but not of its vertical thickness.

The approximation used in Eq. (85) is compared with Noble's plot in Fig. 10.

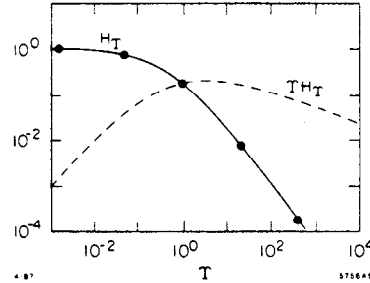


Fig. 10. The beamstrahlung factor  $H_T$  as a function of  $\Upsilon$  as shown by R. Noble (line) and the function used here (dots).

## 6. ROUND VERSUS FLAT BEAMS

A general choice concerns whether we allow the beams to be asymmetrical, i.e., flat. Initially it appears more natural to have round beams, and if we calculate the luminosity for given power in the two cases, we appear to see an advantage.

For round beams ( $R = 1$ ) and fixed beamstrahlung  $\delta$ , using Eqs. (69), (70), (82), (83):

$$\frac{L}{P} \approx \frac{f(\delta, \gamma, \sigma_x)}{(\epsilon_n \beta^*)^{1/2}} H_x H_y, \quad (87)$$

which for a reasonable disruption parameter  $D \approx 10$  gives

$$\frac{L}{P} \approx 6.0 \frac{f(\delta, \gamma, \sigma_x)}{(\epsilon_n \beta^*)^{1/2}}. \quad (88)$$

For flat beams,  $R \gg 1$ , we find:

$$\frac{L}{P} \approx \frac{1}{2} \frac{f(\delta, \gamma, \sigma_x)}{(\epsilon_n \beta^*)^{1/2}} H_y. \quad (89)$$

The factor of 1/2 comes from the term  $2/[1 + (\sigma_x'/\sigma_y')]$  in Eq. (82). This term goes to one for round beams but two for flat beams. The absence of  $H_x$  reflects that for a flat beam negligible disruption can be obtained in the horizontal direction. For  $D_y \approx 10$ , then  $H_y \approx \sqrt{6.0}$  and

$$\frac{L}{P} \approx 1.22 \frac{f(\delta, \gamma, \sigma_x)}{(\epsilon_{ny} \beta_y^*)^{1/2}}, \quad (90)$$

and we see that for the same emittance and final  $\beta^*$  we have lost a factor of five in luminosity for given power.

However, it turns out that there are a number of rather strong advantages in the asymmetric case that can overcome this initial disadvantage.

- 1) Damping rings are naturally asymmetric. Without mixing the vertical emittance would damp to zero. It is quite reasonable to assume mixing of only about 1%, thus giving a much smaller vertical emittance.
- 2) In an RF structure the round irises could be replaced by ellipses or slots with greatly reduced transverse wake fields in one direction, thus allowing the transport of an asymmetrical beam without blowing up its small vertical emittance.
- 3) The chromatic correction section prior to the final forms will involve dipole magnets that will, through synchrotron radiation, blow up the beam emittance. But this blow up will occur in only one direction. A very small vertical emittance need not put additional constraints on the design.
- 4) The final focus, if it uses conventional quadrupoles is intrinsically asymmetrical. With a quadrupole it is easy to focus in one direction if we do not worry about the other. Much weaker focusing is possible if symmetry is required.
- 5) At the final intersection point for fixed  $\delta$  with round beams we have [from Eq. (87)]

$$\frac{L}{P} \propto \frac{1}{(\epsilon_n \beta^*)^{1/2}}. \quad (91)$$

But we also find, again assuming fixed  $\delta$ ,

$$N \propto (\epsilon_n \beta^*)^{1/2}, \quad (92)$$

so high luminosity can only be obtained for small numbers of particles per bunch, which require for reasonable efficiency low accelerating wavelength and serious wake field effects.

With flat beams, Eq. (91) becomes

$$\frac{L}{P} \propto \frac{1}{(\epsilon_{ny} \beta_y^*)^{1/2}} \quad (93)$$

But Eq. (92) is now:

$$N \propto (\epsilon_{nz} \beta_z^*)^{1/2} \quad (94)$$

The two equations are now decoupled and we are free to keep  $N$ , and thus the wavelength, up by keeping  $(\epsilon_{nz} \beta_z^*) > (\epsilon_{ny} \beta_y^*)$ .

- 6) The final advantage in using a flat beam is that it allows a finite angle crossing at the intersection point. With zero angle crossing the quadrupole apertures have to be made large enough to accept the disrupted particles from the oncoming beam. In practice this angle is far larger than that taken up by the initial beam. With finite angle crossing we arrange that the disrupted beam passes outside the opposite final quadrupole. Thus the quadrupole aperture can be set by the incoming beam size. As a result of the smaller aperture requirement, the field gradient can be larger and the focusing strength greater.

In the following section the choice of parameters for a flat beam case will be discussed in detail. The luminosity obtained is  $10^{33}$ . A similar procedure was followed for a round beam case, but the final luminosity achieved was only of the order of  $10^{32}$ , a full order of magnitude less than for a comparable flat beam example. An approximate breakdown of the contributions to this difference is given below:

	<u>Loss/Gain</u>
<u>Losses</u>	
(1) from L/P calculation for fixed $\delta$	1/2
(2) from loss of horizontal enhancement $H_x$	1/2
<u>Gains</u>	
(1) from asymmetric damping ring	× 3
(2) from use of quadrupole focusing	× 2
(3) from finite angle crossing	× 2
(4) from use of larger $N$	× 2
(5) from use of higher group velocity structure	× 2
<u>Net Gain</u>	<u>≈ 12</u>

## 7. PARAMETER CHOICES

### 7.1 Introduction

In the above sections we have discussed each of the collider components separately. We have noted, however, that in many cases the requirements of one component conflict with those of another. I will discuss these conflicts one-by-one, although the interwoven nature of the problem generates difficulty in selecting the order. In each case, I will attempt to suggest reasonable choices and thus obtain an example parameter list.

I will leave discussion of the wavelength to the next section. Here I will attempt to make choices that will be reasonably independent of wavelength.

The energy of the collider studied will be

$$E_{c.of.m} = .5 + .5 \text{ TeV} \quad (95a)$$

## 7.2 Accelerating Gradient

A high gradient will reduce the overall length of the accelerator and may be expected to reduce a linear component of its cost. However, a higher accelerating gradient will imply a higher stored energy and higher costs associated with the RF power supply. The best gradient to minimize costs will then depend on the relative linear and stored energy related costs. An upper bound will exist on the acceleration gradient set by breakdown, excessive heating or beam deflections due to uncontrolled field emission in the structure.

Figure 11 illustrates a) the estimated limits [15] on accelerating gradient, and b) estimated lines of constant cost for both linear and stored energy costs. In both cases the dependence is shown as a function of the accelerating gradient and wavelength. The assumptions were:

Linear cost per meter	$C_l \approx 40 \text{ K\$/m}$	
RF source cost per Joule	$C_j \approx 2.4 \text{ K\$/J}$	(Sec. 8.5)
group velocity	$\beta_g \approx .08 c$	(Sec. 7.3)
fill time/attenuation time	$\tau \approx .25$	(Sec. 7.4)
average accelerating gradient/max	$\eta_a \approx 0.8$	

With these assumptions the linear cost

$$\$l \approx \frac{5 \times 10^{10}}{\mathcal{E}_a \text{ (MeV/m)}} \quad (95b)$$

and the RF energy cost

$$\$_{RF} = C_j \frac{\mathcal{E}_a^2}{s_t} \cdot \left( \frac{E}{\mathcal{E}_a} \right) \frac{1}{\eta_a} \quad (96)$$

which with the above assumptions gives

$$\$_{RF} \approx 7.4 \times 10^5 \lambda \text{ (cm)}^2 \mathcal{E}_a \text{ (MeV/m)} \quad (97)$$

The minimum cost will then be for an accelerating gradient

$$\mathcal{E}_a \text{ (min. cost)} \approx \frac{260 \text{ MeV/m}}{\lambda \text{ (cm)}} \quad (98)$$

This relation is also illustrated in Fig. 11. At this gradient, the accelerator and power source would cost would be:

$$\$l + \$_{RF} \approx .38 \lambda \text{ (cm)} \text{ (B\$)} \quad (99)$$

The numerical constant in Eqs. (98) and (99) should not be taken too seriously, but are probably accurate enough to indicate that for any reasonable choice of wavelength (i.e.,  $\lambda \geq 1 \text{ cm}$ ), the optimum accelerating gradient is well below the estimated maximum gradient. Costs will not be lowered by higher acceleration gradients unless one first finds ways to lower the power source costs.

High accelerating gradients can be imperative if there is a limitation in the length at a particular site. At SLAC, for instance, the longest linear collider possible is about 7 km. If a center-of-mass energy

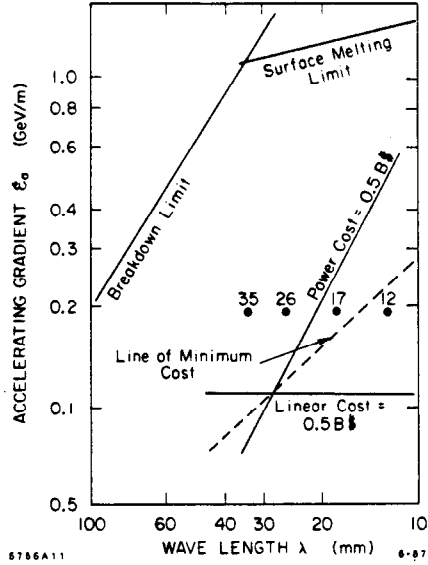


Fig. 11. Lines of constant cost for 1) RF power, and 2) length of accelerator, as a function of accelerating gradient and wavelength. The dotted line indicates accelerating gradients chosen to minimize overall cost. Breakdown and surface melting limits on accelerating gradient are also given.

of 1 TeV is required and allowances are made for phase advance, filling factors, etc., then a reasonable minimum gradient will be

$$\boxed{\epsilon_a = 186 \text{ MeV/m}} \quad (100)$$

From Eq. (98) one sees that this choice is at the estimated value for minimum cost if the wavelength were fixed at

$$\lambda \approx 14 \text{ mm} \quad (101)$$

and we will, in fact, be considering wavelengths of this order of magnitude. Thus, for our examples it will not be unreasonable to use the assumption of Eq. (100).

### 7.3 RF Structure Group Velocity

In Eq. (99) we see that the stored energy and cost of a collider is related to the wavelength; but a shorter wavelength in general implies a smaller iris hole, and a smaller iris hole will cause larger wakefields that give all kinds of problems. For short bunches these wakefields are dependent primarily on the iris radius 'a' and only weakly on the wavelength. We can thus assume that the wakefield problems imply a bound only on 'a' and not on 'λ'.

For a given value of 'a' the RF energy required per meter is given by Eqs. (21)-(27).

$$w_{RF} = \frac{\epsilon_a^2 a^2}{8\pi \eta \rho} \quad (102)$$

where the dependence on the group velocity  $\beta_g$  is contained in the normalized and corrected elastance  $s_{at}$  which is plotted against the group velocity in Fig. 2b.

The dependence shown is, of course, dependent on the particular choice of accelerating structure considered (in this case a SLAC-like iris loaded cylindrical structure with  $2\pi/3$  phase advance per cell).

The elastance is seen to rise (and thus the required RF energy to fall) monotonically with increasing group velocity. But if a higher group velocity is chosen, the peak electron field within the cavity ( $\mathcal{E}_{pk}$ ) rises (see Fig. 2d). (The RF instantaneous power  $P_{RF}$  also rises, but not seriously). From Fig. 11 we might conclude that the higher fields in the cavity are not a problem, but some reasonable compromise must still be made. For this example I will select

$$\beta_g = .08 \quad (103)$$

which gives

$$\frac{\mathcal{E}_{pk}}{\mathcal{E}_a} \approx 2.6 \quad , \quad (104)$$

$$s_{at} \approx 21 \times 10^9 \text{ VmC}^{-1} \quad . \quad (105)$$

#### 7.4 Fill Time

From Eq. (27) we see that the RF energy required depends on the parameter  $\tau$ :

$$w_{RF} \propto \frac{1}{\eta_\rho} = \frac{\tau^2}{(1 - \exp(-\tau))^2} \quad , \quad (106)$$

$$\tau = \frac{T}{T_0} \quad ,$$

where  $T$  is the fill time and  $T_0$  the attenuation time. For  $\tau \ll 1$  then approximately

$$w_{RF} \propto (1 + \tau) \quad , \quad (107)$$

$$P_{RF} \propto \frac{1 + \tau}{\tau} \quad , \quad (108)$$

A compromise must be reached between the stored energy  $w_{RF}$  that falls with  $\tau$  and the peak power  $P_{RF}$  that rises (see Fig. 12). For this example I take

$$\tau = .25 \quad , \quad (109)$$

yielding

$$\eta_\rho = .783 \quad . \quad (110)$$

#### 7.5 Damping Ring Impedance $Z/n$

From Eqs. (2) and (3) we found that the equilibrium emittance of a damping ring will always be lower if  $Q$ , the tune, can be raised. But from Eqs. (10) and (12) we also found that a high tune implied a small  $\alpha$  and correspondingly smaller impedance requirement  $Z/n$ .

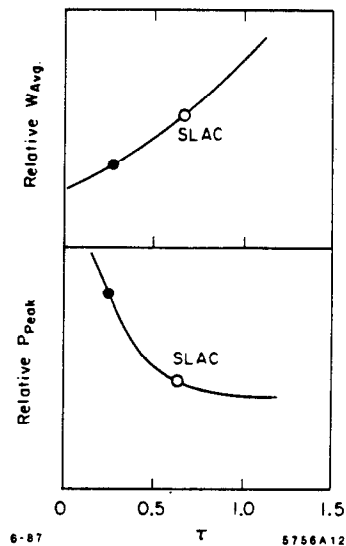


Fig. 12. Average and peak power requirements as a function of the fill time parameter  $\tau$ .  $\tau = \text{fill time/attenuation time}$ .

As a rough constraint on the allowable tune, I assume

$$\frac{z}{\pi} \geq .5 \Omega \quad (111)$$

#### 7.6 Emittance Ratio $\epsilon_x/\epsilon_y$

In the absence of intrabeam scattering, the vertical emittance in a damping ring with no mixing would go to zero. It is clearly desirable to use this simple fact. The limit will be set by how low a mixing can be obtained. For all flat beam cases, I have chosen 1% as a reasonable aim for this mixing, and thus

$$\frac{\epsilon_x}{\epsilon_y} = 100 \quad (112)$$

One should note that we do not gain the full factor of 100. The lower vertical emittance increases the intrabeam scattering and increases the  $\epsilon_x$ . However, a gain of at least  $\sqrt{100}$  is obtainable since if  $\epsilon_x$  is increased by this and thus intrabeam scattering will remain the same.

#### 7.7 Final Focus Pole Tip Field

We will see from our examples that the required quadrupole apertures are very small (of the order of .2 mm diameter). Under these circumstances it is not reasonable to use superconducting coils. Pulsed magnets could be built to these dimensions but it would be hard to avoid mechanical motions (the quads need to be steady to a few  $\text{\AA}$ ). For these reasons, I am assuming that conventional iron quads are employed and limit the pole tip fields to

$$B = 1.4 \text{ Tesla} \quad (113)$$

### 7.8 Crossing Angle

With finite angle crossing we wish the oncoming disrupted beam to pass well clear of the final quadrupole. If I assume negligible beam at six times the calculated maximum disruption angle, then the full crossing angle  $\theta_c$  must be

$$\theta_c \geq 6 \theta_{Dz} + \theta_{Qz} \quad , \quad (114)$$

where  $\theta_Q$  is the angle subtended by the outside of the final quadrupole. However, a quadrupole can be left open on its sides (see Fig. 13) and thus, providing the vertical disrupted size  $\theta_{Dy}$  is small,  $\theta_{Qz}$  can be zero. Nevertheless, some allowance for the quadrupole is needed and for these calculations I have assumed

$$\theta_c = 12 \theta_{Dz} \quad . \quad (115)$$

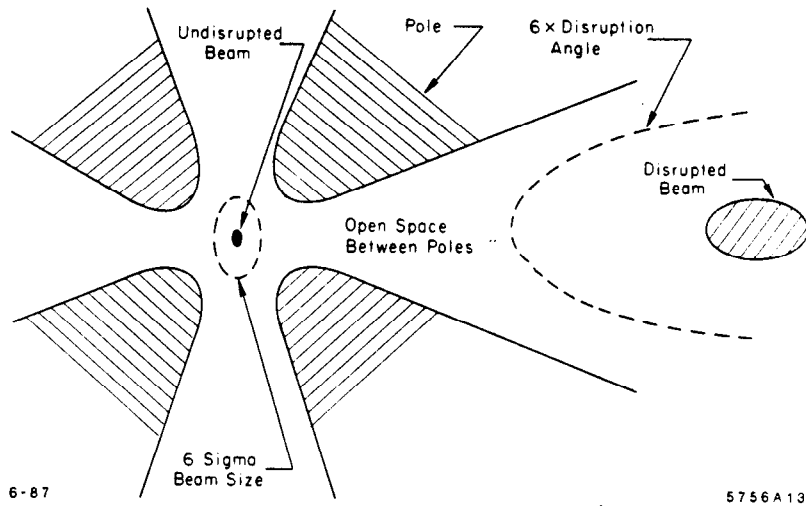


Fig. 13. Cross section at the start of the first final focus quadrupole showing incoming and disrupted beams.

A luminosity loss will occur if this angle is small compared to the angle of the diagonal of the bunch, i.e., we require

$$\theta_c < \theta_{diag} = \frac{\sigma_z}{\sigma_x} \quad . \quad (116)$$

### 7.9 Particles per Bunch $N$

Having fixed the wavelength, iris hole diameter and accelerating gradient we can now choose the number of particles per bunch and thus the loading ( $\eta$ ) of the cavity, defined by

$$\eta = Nes \propto \frac{N}{\lambda^2} \quad , \quad (117)$$

where  $s$  is the elastance [see Eq. (25)].  $\eta$  represents the fraction of energy stored in the cavity that is transferred to the bunch. Common sense would indicate that a higher  $\eta$  will give a higher luminosity, but it is more complicated.

The luminosity [from Eqs. (69) and (70)], for fixed  $\epsilon_x/\epsilon_y$  and  $\beta_x/\beta_y$  is:

$$\mathcal{L} \propto \frac{N^2}{\epsilon \beta^*} \quad (118)$$

But from Eq. (3) the emittance, if limited by intrabeam scattering, is

$$\epsilon \propto N^{1/2} \quad (119)$$

From Eqs. (52) and (55) the uncorrectable momentum spread

$$\sigma_p \geq s\sigma_p \propto N \quad (120)$$

Using Eq. (66) we have for the final focus

$$\beta^* \propto \sigma_p^2 \theta_{\text{beam}} \quad (121a)$$

$$\theta_{\text{beam}} \propto \left(\frac{\epsilon}{\beta^*}\right)^{1/2} \quad (121b)$$

so

$$\beta^* \propto \sigma_p^{4/3} \epsilon^{1/3} \propto N^{4/3} N^{1/6} \propto N^{3/2} \quad (121c)$$

Combining Eqs. (118), (119) and (121c):

$$\mathcal{L} \propto \frac{N^2}{N^{1/2} N^{3/2}} = \text{constant} \quad (122)$$

*i.e.*, when we work it through we find the luminosity is not dependent on  $N$  or  $\eta$ !

The above is only true if the final focus is indeed limited by momentum spread. If the momentum spread is too small, the tolerance requirements will become excessive and the dependence of Eq. (122) will fail. A not unreasonable lower bound on  $\sigma_p(\text{focus})$  is taken at about one third of the SLC value; *i.e.*, we assume Eq. (121c) valid only if

$$\sigma_p(\text{focus}) \geq 0.15\% \quad (123)$$

This momentum spread can come either from wakefield effects [ $\sigma_p(\text{wake})$ ] or from the intrinsic longitudinal emittance of the beam [ $\sigma_p(\text{emittance})$ ]. If we fix these relative contributions, *e.g.*, if

$$\frac{\sigma_p(\text{emittance})}{\sigma_p(\text{wake})} = 0.7 \quad (124)$$

then

$$\begin{aligned} \sigma_p(\text{wake}) &\geq \frac{\sigma_p(\text{focus})}{\sqrt{1+0.7^2}} = \frac{.15\%}{\sqrt{1+0.7^2}} \\ &\approx .12\% \end{aligned} \quad (125)$$

Given the other assumptions on iris diameter and bunch length, the above requirement on the longitudinal wake can be interpreted as a bound on the loading parameter  $\eta$

$$\eta \geq 1.2\% \quad (126)$$

It could be tempting to choose a larger loading if it were not for another constraint. The momentum spread needed for Landau damping is also proportional to  $N$  [from Eqs. (36) and (33)]

$$\sigma_p(\text{Landau}) \propto N \left( \frac{\sigma_x}{\lambda^4} \right) \beta_{\text{linac}}^2, \quad (127)$$

and the distance to remove this momentum spread [from Eq. (39)]

$$\ell_c \propto \frac{\sigma_p \lambda}{\sigma_x}. \quad (128)$$

Thus

$$\ell_c \propto N \beta_{\text{linac}}^2 \lambda^{-3}. \quad (129)$$

Now from Eq. (31)

$$\beta_{\text{linac}}^2 \propto a \propto \lambda, \quad (130a)$$

so

$$\sigma_p(\text{Landau}) \propto \frac{N}{\lambda^2} \cdot \frac{\sigma_x}{\lambda}, \quad (130b)$$

and thus for fixed  $\sigma_x/\lambda$  (see Section 7.10)

$$\ell_c \propto \frac{N}{\lambda^2} \propto \eta. \quad (130c)$$

So a high value of  $\eta$  implies a long distance needed to fix the Landau damping momentum spread. In our example we find if  $\eta = 1.2\%$ , then  $\ell_c \approx 200$  m which is already rather long. I therefore select,

$$\boxed{\eta \approx 1.2\%} \quad (131)$$

#### 7.10 Bunch Length $\sigma_x$

The bunch length is a very sensitive parameter and must satisfy many simultaneous conditions. It does not, however, for our energy machine, have much effect on the beamstrahlung.

At low energies, when  $\Upsilon \ll 1$  [see Eq. (86)], then the beamstrahlung parameter [Eq. (82)]

$$\delta \propto \sigma_x^{-1}. \quad (132a)$$

At higher energies when the parameter  $\Upsilon \gg 1$ , then the beamstrahlung parameter [from (82), (85) and (86)]

$$\delta \propto \sigma_x^{1/3}. \quad (132b)$$

But in the energy region about .5 TeV we find that for  $\sigma_x$  between  $5 \mu$  and  $100 \mu$ , the beamstrahlung is rather independent of  $\sigma_x$  (see Fig. 10).

$\sigma_x$  does, however, effect other things. It should be kept small because

- (1) Luminosity is lost when  $\sigma_x \approx \beta_y^*$ , or larger.

(2) Luminosity is lost if  $(\sigma_x/\sigma_z) \approx \theta_{\text{crossing}}$ , or larger.

(3) Transverse wakes  $\propto \sigma_x$ .

(4) The disruption parameter  $D \propto \sigma_x$ , and instabilities may occur if the disruption parameter  $D$  is much larger than ten.

However  $\sigma_x$  should be kept large because

(1) For fixed momentum spread a small  $\sigma_x$  implies a small longitudinal emittance  $\epsilon_x$  which will increase the equilibrium emittance in the damping ring  $\epsilon_y$  by Eq. (3). It should also not deviate too far from a convention value of the order of .02 m, or else the RF necessary to obtain the needed long bunch length becomes difficult.

(2) If  $\sigma_x$  is too small, the disruption parameter  $D$  could fall below two, and the disruption enhancement would be lost.

(3) If  $\sigma_x$  is large, it is harder to correct the longitudinal momentum spread in the linac.

It is this last constraint that seems to limit how small  $\sigma_x$  can be, so I will discuss it further. The first order momentum spread from the longitudinal wake, for short bunches, is approximately [Eqs. (48), (53), (54) and (117)]

$$\sigma_p(\text{wake}) \propto \frac{N}{a^2} \propto \frac{N}{\lambda^2} \propto \eta \quad (133)$$

The momentum spread required for Landau damping, from Eq. (130b),

$$\sigma_p(\text{Landau}) \propto \eta \frac{\sigma_x}{\lambda} \quad (134)$$

The phase to maintain the spread required for Landau damping is thus

$$\begin{aligned} \tan \theta &\propto \frac{\lambda}{\sigma_x} [\sigma_p(\text{wake}) - \sigma_p(\text{Landau})] \\ &\propto \frac{\lambda}{\sigma_x} \left( \eta - \text{constant} \frac{\sigma_x}{\lambda} \right) \\ &\propto \eta \left( \frac{\lambda}{\sigma_x} \right) - \text{constant} \end{aligned} \quad (135)$$

If we require that the accelerator length is not increased by more than 10%, then

$$\cos \theta \geq .9 \quad (136)$$

which, with the other assumptions, gives

$$\boxed{\frac{\sigma_x}{\lambda} \approx 1.5 \times 10^{-3}} \quad (137)$$

### 7.11 Linac Focusing

The transverse wake blow up of transverse emittance can be controlled by the introduction of a

longitudinal momentum spread  $\sigma_p$ (Landau) where [Eq. (36)]

$$\sigma_p(\text{Landau}) \propto \frac{\partial W_t}{\partial z} \sigma_x N \beta^2 , \quad (138)$$

where  $\beta$  is the average focus strength in the linac. In order to keep  $\sigma_p$  small, it is desirable to have as small a  $\beta$  as possible. I assume we use quadrupoles with the least possible pole tip radius and place the quads between accelerator sections. I assume

$$\begin{aligned} \text{a(quadrupole)} &= 1.26 \text{ a (iris)} && \text{(as at SLAC)} \\ \text{quadrupole fraction of } \ell &= 5\% \\ \text{quadrupole pole tip field} &= 1.4 \text{ Tesla} \\ \text{phase advance per cell} &= 90^\circ \end{aligned} \quad (139)$$

From the above and from Eq. (31)

$$\beta \propto \sqrt{a} \propto \sqrt{\lambda} . \quad (140)$$

From Eq. (33)

$$\frac{\partial W_t}{\partial z} \propto \frac{1}{\lambda^4} , \quad (141)$$

from Eq. (137)

$$\sigma_x \propto \lambda , \quad (142)$$

from Eq. (126) and (117)

$$N \propto \lambda^2 . \quad (143)$$

We have

$$\sigma_p(\text{Landau}) \propto \frac{1}{\lambda^4} \lambda \lambda^2 (\sqrt{\lambda})^2 = \text{constant} , \quad (144)$$

and one finds that the momentum spread for Landau damping is independent of  $\lambda$ . In our case

$$\sigma_p \approx .8 \times 10^{-3} . \quad (145)$$

#### 7.12 Focus Asymmetry $\beta_x^*/\beta_y^*$

In Section 7.7 we specified the final focus maximum pole tip field, and using Eq. (66) we can determine the minimum  $\beta_y^*$  assuming that the quadrupole aperture is determined by the vertical beam size  $\theta_y$ . It is important that the aperture is not determined by the horizontal beam size or else the  $\beta_y^*$  will be compromised and the luminosity obtainable for given beamstrahlung will be reduced [see Section 6 and Eq. (90)]. In order to assure this we must choose a sufficiently high ratio of  $\beta_x^*/\beta_y^*$ .

We note that the ratio of beam divergence angles at the intersections will be

$$\frac{\theta_x}{\theta_y} = \left( \frac{\epsilon_x}{\epsilon_y} \cdot \frac{\beta_y^*}{\beta_x^*} \right)^{1/2} . \quad (146)$$

For the flat beam cases the ratio of required aperture in the final focus is greater than this because of the natural asymmetry of the quadrupole system

$$\frac{a_x}{a_y} = \frac{A_x}{A_y} \cdot \frac{\theta_x}{\theta_y} \approx 1.8 \left( \frac{\epsilon_x}{\epsilon_y} \cdot \frac{\beta_y^*}{\beta_x^*} \right)^{1/2} . \quad (147)$$

We require that

$$\frac{a_z}{a_y} \leq 1 \quad , \quad (148)$$

and thus

$$\frac{\beta_z^*}{\beta_y^*} \geq (1.8)^2 \frac{\epsilon_z}{\epsilon_y} \quad . \quad (149)$$

Since in Section 7.5 we selected  $\epsilon_z/\epsilon_y = 100$  we obtain

$$\frac{\beta_z^*}{\beta_y^*} \geq 324 \quad . \quad (150)$$

Higher values could be used and would reduce the beamstrahlung, if that were required, but 324 is already a large asymmetry and the use of an even larger value would probably introduce tolerance problems. Thus I will use:

$$\boxed{\frac{\beta_z^*}{\beta_y^*} = 324} \quad . \quad (151)$$

### 7.13 Wall Power

In the designs being considered, there is no strong constraint on the repetition rate except for the overall average power consumption. For these examples, I have assumed

$$\boxed{\text{Wall Power} = 100 \text{ MWatts}} \quad , \quad (152)$$

There is no strong justification for this choice. It should depend on electrical power cost, potential running time per year and some reasonableness criterion. Double the power will double the luminosity and repetition rate, and ease the vibration requirements.

I will assume the RF power source efficiency.

$$\boxed{\text{RF power source efficiency} = 36\%} \quad , \quad (153)$$

as estimated for a relativistic klystron (see Section 8.5).

## 8. CHOICE OF WAVELENGTH

### 8.1 Introduction

I have, using the assumptions of Section 7, generated parameter sets for different wavelengths

$$\begin{aligned} \lambda &= 35.01 \text{ mm} & (8.56 \text{ GHz} = 3 \times \text{SLAC}) \\ \lambda &= 26.26 \text{ mm} & (11.42 \text{ GHz} = 4 \times \text{SLAC}) \\ \lambda &= 17.51 \text{ mm} & (14.14 \text{ GHz} = 6 \times \text{SLAC}) \\ \lambda &= 11.67 \text{ mm} & (25.70 \text{ GHz} = 9 \times \text{SLAC}) \end{aligned}$$

These parameter lists are given in full in Appendices I and II. Here I will examine different aspects of these parameters in turn, and note relative advantages and disadvantages.

## 8.2 Luminosity and Beamstrahlung

Figure 14 shows lines of possible combinations of luminosity and beamstrahlung for the four wavelengths. In each case the standard solution is given by the dot. Higher beamstrahlung is obtained if  $\beta_z^*/\beta_v^*$  is chosen to be less than that given in Section 7.12, but no gain in luminosity is obtained—a futile exercise. Lower beamstrahlung can be obtained by lowering the number of particles per bunch (as indicated in the figure), but in these cases I have assumed that neither the focus or damping rings are modified and that no advantage is taken from the lower wakefields and impedance requirements. I am assuming that other limits now apply (see discussion in Section 7.9).

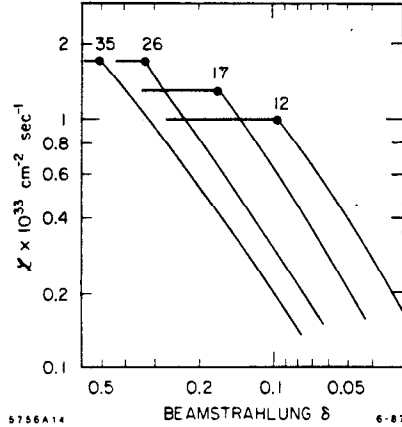


Fig. 14. Luminosity versus beamstrahlung for different wavelength solutions.

Figure 15 shows the peak luminosity and luminosity at  $\delta = .1$ , as a function of the wavelength. At wavelengths above 20 mm there is little gain in maximum luminosity and a big loss in luminosity at fixed  $\delta$ . Below 20 mm the peak luminosity falls significantly, but the luminosity at low beamstrahlung rises. I would conclude from these considerations

$$10 \text{ mm} \leq \lambda \leq 20 \text{ mm} \quad (154)$$

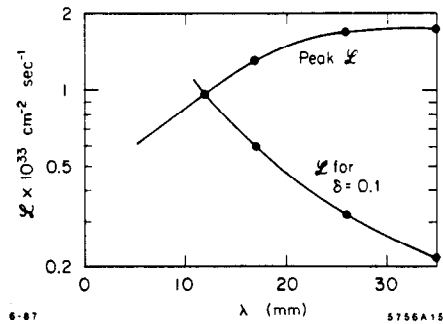


Fig. 15. Peak luminosity and luminosity at fixed beamstrahlung, as a function of the wavelength chosen.

### 8.3 Final Focus Criteria

In Section 7.10 in discussing the bunch length choice, a number of criteria were listed, but only one used. Three of these concerned the final focus and I now examine how well these are satisfied (see Table I).

**TABLE I.**

Criterion	Wavelength (mm)			
	35	26	17	12
$\frac{\sigma_z}{\beta^*} < 1$	(1.08)	.85	.61	48
$\frac{\theta_{\text{cross}}}{\theta_{\text{diag}}} < 1$	(1.18)	.69	.3	15
$3 < D < 10$	(23)	(14)	6	3

We see here that though all these criteria are well satisfied for the 17 mm and 12 mm cases, they are violated for 35 mm and only marginal for 26 mm. I thus conclude

$$\lambda \leq 20 \text{ mm} \quad (155a)$$

To avoid the loss of a disruption enhancement when  $D < 3$ , we also need

$$\lambda \geq 12 \text{ mm} \quad (155b)$$

Another criterion concerns the possible need to use a dipole field to sweep low momentum disrupted electrons away from the first quadrupole (see Section 5.2). The length required for this should certainly be less than the space available. With the assumptions made, see Table II.

**TABLE II.**

Criterion		Wavelength (mm)			
		35	26	17	12
Length to first quad (m)	$l_1$	.47	.43	.39	.35
Length to sweep (m)	$l_{\text{sweep}}$	(.84)	(.56)	.30	17

Once again, the requirement is violated for the two longer wavelength examples and we require

$$\lambda \leq 20 \text{ mm} \quad (156)$$

### 8.4 Tolerances

Two kinds of tolerance have been defined in Section 3.3.

- a) Alignment tolerances can be satisfied if beam position monitors have accuracy significantly below the tolerance and if feedback is employed to control the average orbit. The values of tolerance required are calculated [using Eq. (40)] and shown in Table III below.

The requirements are significantly more severe for the short wavelength examples than for the longer wavelength cases.

These alignment requirements can be relieved by the use of elliptical irises. In the 12 mm case the calculated tolerance is only 160  $\mu$  with a 2:1 elliptical iris—but the use of such asymmetric structures is another subject. But, larger wavelengths are still preferred, and if we require tolerances greater than 50  $\mu$ , we obtain:

$$\lambda \geq 15 \text{ mm} \quad (157)$$

- b) The second kind of tolerance concerns vibration. Any linac quadrupole motion that occurs between one pulse and the next cannot be corrected, even if it can be measured. From Eq. (47) the rms allowable random motion from one pulse to the next is also given in Table III, below.

TABLE III.

Criterion	Wavelength (mm)			
	35	26	17	12
Beam size $\sigma_y$ ( $\mu$ )	.93	.77	.60	.45
Number of quads $N_q$	336	387	478	579
Alignment tolerance $\langle \Delta_y \rangle_a$ ( $\mu$ )	122	93	66	44
Vibration tolerance $\langle \Delta_y \rangle_v$ ( $\mu$ )	.02	.016	.011	.008
$f$ (Hz)	55	100	220	500
$\langle \Delta_y \rangle_{\text{ground}}$ ( $\mu$ )	.002	.001	.0005	.0002
$\langle \Delta_y \rangle_{\text{tolerance}} / \langle \Delta_y \rangle_{\text{ground}}$	10	16	22	40

We note again that this tolerance is more stringent for the short wavelength cases than for the long wavelength case. However, the repetition frequency  $f$  is higher for the short wavelength cases and thus serving is easier. If, for instance, we look at a typical ground vibration [16], we see that the amplitudes at high frequencies are much smaller than at lower frequencies. As a result the ratio of tolerance to ground vibration is better for the short wavelength examples, so a small wavelength is preferred.

It may, however, be noted that the ground vibration is in all cases less than the tolerance, so there is no real constraint on the wavelength.

### 8.5 Damping Ring Criteria

Some of the damping ring parameters for the different wavelength solutions are shown in Table IV.

TABLE IV.

Criterion	Wavelength (mm)			
	35	26	17	12
Horizontal emittance ( $10^{-6}$ m) $\epsilon_x$	4.4	3.5	2.5	1.8
Long emittance (m) $\epsilon_x$	.044	.033	.022	.015
Bunch length (cm) $\sigma_x$	3.4	2.4	1.5	1.0
Ring radius (m) $R$	12.3	14.6	18.2	23.3
Tune (Horizontal) $Q_x$	18	21	25	32
Impedance ( $\Omega$ ) $Z$	183	300	600	1200

The lower wavelength solutions require damping rings with lower emittance, obtained because of the lower number of particles per bunch. As a consequence, however, the low wavelength cases require larger diameter, higher tune, and will be more costly and have tighter tolerances.

On the other hand, we note that the solutions with longer wavelength involve relatively large longitudinal emittance and correspondingly long bunches. This in turn will mean very low frequency RF systems that may be large, more costly, and possibly more of an impedance problem. This problem is compounded because the impedance requirement for the full ring (even though  $Z/n$  is the same for all cases) is far more severe for the long wavelength cases.

On balance, the shorter wavelength solutions are probably more reasonable. If I require a bunch length less than 2 cm, I obtain

$$\lambda \leq 24 \text{ mm} \quad (158)$$

### 8.6 RF Power Source Cost

If we assume that the linac is filled by an induction linac powered relativistic klystron then we are in a position to make a very rough first guess at the cost. Let us assume that the induction linac is of the type now operating at Livermore. It would then consist of some multiples of klystron units consisting of

1	DC power supply	(50 K\$)
1	880 Joule, 1 $\mu$ sec, modulator	(80 K\$)
1	Magnetic compressor	(175K \$)
3	2 KA induction units	(500K \$)
	Focusing magnets	(50K \$)
	Bunching and extraction cavities	(100K \$)

I do not wish to rule out the Two-Beam Accelerator concept in which the klystron beam is reaccelerated, and energy extracted, many times. In such a case the "klystrons" referred to here would be merely added together. No large cost differential would be expected.

Such a system might be expected to have an overall efficiency of 36% (modulator 90%, induction linac 90%, fraction of pulse flat 66%, klystron energy extraction 66%). The energy out would then be 320 Joules.

The costs listed above are those given by Dan Birx for the construction of single units; they do not include engineering, overhead or contingency costs.

If I assume a factor of 1.6 to cover these extra expenses, but allow a 50% cost reduction from mass production then I obtain a cost per output Joule of

$$\$/\text{Joule} = \frac{760 \text{ K\$}}{320 \text{ J}} = 2.4 \text{ K\$/Joule} \quad (160)$$

The Livermore design, with minor modifications, could deliver an RF pulse length anywhere between 100 nsec to  $\sim 14$  nsec, without significant cost differential (a 10% increase could be incurred for  $t \leq 25$  nsec to provide a ferrite instead of metglass final pulse compression stage). A single unit could thus provide peak power between 3.2 GWatts and 21 GWatts without significant cost differential. It is the cost per stored energy that dominates.

Using Eq. (22) and allowing for extra length because of phase advance [Eq. (136)] and the length needed to correct the Landau momentum spread [Eq. (130c)], I now estimate the RF systems required as a function of wavelength in Table V.

Criterion	Wavelength (mm)			
	35	26	17	12
Total stored energy (kJ)	650	370	164	72
Pulse length (nsec)	70	46	25	14
Number of "klystrons" <sup>a)</sup>	2030	1160	512	225
Estimated cost B\$	1.56	.89	.39	.19 <sup>b)</sup>
meters per "klystron" <sup>a)</sup>	3.3	5.9	13.3	30

<sup>a)</sup> number of induction units is approximately three times this.

<sup>b)</sup> including 10% increase to cover possible costs associated with 14 nsec pulse length.

When compared to a possible linear cost for a 7 KM linac of the order of .3B\$, it would appear that the RF costs for both 35 mm and 26 mm wavelengths are excessive (see Fig. 16).

An alternative way of judging what is reasonable or unreasonable is to consider the number of "klystrons" per meter.

For the 35 mm wavelength case we would need a complete unit every 3.3 m. Since each one is about 6 m long, they would have to be arranged side-by-side in a 6-m wide corridor parallel with the entire accelerator. This seems not reasonable.

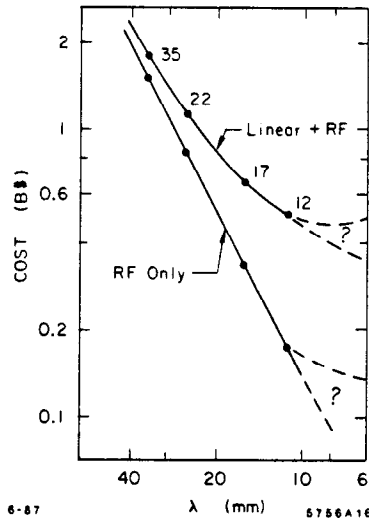


Fig. 16. Cost of RF power supply as a function of the wavelength. Also, this cost together with an assumed linear component. The dotted lines indicate uncertainty in cost estimation in a region of pulse lengths less than 15 nsec.

For the wavelengths less than 17 mm the induction units could be parallel with the main accelerator and take up only a couple of meters of width. Thus from this, or from a requirement that the power source cost no more than the linear cost, we obtain

$$\lambda \leq 17 \text{ mm} \quad (161a)$$

There is, however, an argument against going below 12 mm since pulses of less than 14 nsec have not yet been achieved.

$$\lambda \geq 12 \text{ mm} \quad (161b)$$

## 8.7 Wavelength Conclusion

Reviewing the constraints on wavelength, we have:

Eq. (154)	$10 \text{ mm} \leq \lambda \leq 20 \text{ mm}$
Eq. (155a)	$\lambda \leq 20 \text{ mm}$
Eq. (155b)	$12 \text{ mm} \leq \lambda$
Eq. (156)	$\lambda \leq 20 \text{ mm}$
Eq. (157)	$15 \text{ mm} \leq \lambda$
Eq. (158)	$\lambda \leq 24 \text{ mm}$
Eq. (161a,b)	$17 \text{ mm} \leq \lambda \leq 17 \text{ mm}$

From which we see that the only wavelength that satisfies all conditions is

$$\lambda \approx 17 \text{ mm} \quad .$$

This conclusion should not be interpreted as an exact statement. By adjusting the parameter choices and criteria of Section 7, one could clearly come up with solutions for other wavelengths. But if a wavelength significantly different is required, then some price in luminosity, beamstrahlung, cost, length or other parameter would have to be paid.

## 9. CONCLUSIONS

### 9.1 Warnings

This study has made many assumptions that are uncertain, and in some cases clearly unrealistic. It was not intended to yield a design of a real collider. In particular we note:

- (1) No emittance dilution has been included in the calculation. Finite misalignments, wakefields, synchrotron radiation and higher order aberrations will lower the effective emittances and lower the luminosity for fixed power.
- (2) The Landau damping calculation uses only the two bunch approximation and is not exact.
- (3) The wakefield expressions used may not be correct for the short bunches that the study proposes to use.
- (4) Pulse-to-pulse variations in transverse fields in the accelerating structure may be a severe problem, and it has not been included.

Clearly much more study is required and this work should be taken only as a guide to what may be possible.

## 9.2 Encouragement

On the other hand, this study has left out many features that could make things much better. In particular:

- (1) More than 100 MW could be used, thus giving both more luminosity and repetition rate.
- (2) Asymmetric irises could be employed in the linac to reduce the vertical wakefields and, as a result, reduce the alignment tolerances.
- (3) Higher order chromatic correction in the final focus could probably be employed. Alex Chou [17] has shown that when correction is only required in one direction, octupoles can improve the correction beyond that assumed here.
- (4) Super disruption [18] is a concept that uses two closely spaced bunches, so that the first acts to focus particles of the second bunch and gives an increase in luminosity. In our case, two bunches would not be practical, but shaping of the bunches (the front should have a larger radius than the back) could probably help.
- (5) Longitudinal shaping of the bunch would lower the uncorrectable third order momentum spread and help the final focus.
- (6) Other focus schemes using plasmas or other high field magnets could lower the final focus  $\beta^*$ .
- (7) The use of RF focussing elements in the linac or final focus could eliminate the need for a Landau momentum spread correction section. This idea is being studied at CERN [19].
- (8) Multiple bunches in the linac could dramatically increase the beam current and luminosity. The long term transverse wakefields make this impossible with a conventional cavity, but studies are underway on cavities that would damp the transverse modes and allow such operation.

## 10. FINAL REMARKS

This study, with many assumptions, has generated a self-consistent and semi-conventional parameter list for a .5 on .5 TeV  $e^+e^-$  collider with a luminosity above  $10^{33} \text{ cm}^{-2} \text{ sec}^{-1}$ . It is true that many of the assumptions are optimistic (see Section 9.1), but it is also true that many ideas were not included that could make things much better (see Section 9.2). On balance, I believe the study is very encouraging.

Much work remains to be done, but I believe now that a collider with the proposed specification can be built in the not too distant future. The physics potentials of such a facility are well known. The relative ease of performing experiments with such a machine compared with the difficulties of working with such luminosities in a hadron collider have frequently been noted.

For these reasons, and because of the physics differences, electron positron colliders have always complimented hadron machines operating in a similar energy regime. The collider described here certainly approaches the regime of the SSC and would be an appropriate compliment to it. One hopes that the remaining uncertainties can be resolved and a proposal can soon be made for the construction of such a facility.

I would like to thank the many members of the groups at SLAC, CERN, KEK, LBL and Livermore who have contributed to these studies. In particular, I would thank C. Bane, K. Brown, D. Farkas, R. Ruth, and P. Wilson at SLAC for their many contributions and help in this work.

#### REFERENCES

1. K. Steffen, "The Wiggler Storage Ring," Internal Report DESY PET 79/05 (1979).
2. R. Palmer, "Cooling Rings for TeV Colliders," SLAC-PUB-3883 (1985), Proc. Seminar on New Techniques for Future Accelerators, Erice, Italy, May 11-17, 1986.
3. M. Sands, "The Physics of Storage Rings," SLAC-PUB-121 (1979), p. 110.
4. J. Bisognano et al., "Feasibility Study of Storage Ring for a High Power XUV Free Electron Laser," LBL-19771 (1985). [Note that the factor four in Eq. (6) is missing in both this reference and Ref. 4.]
5. Z. D. Farkas, P. B. Wilson, "Comparison of High Group Velocity Accelerating Structures," SLAC-PUB-4088 (1987).
6. P. B. Wilson, "Linear Accelerators for TeV Colliders," SLAC-PUB-3674 (1985); Proc. 2nd Workshop on Laser Acceleration, Malibu, CA, AIP Conf. Proc. 130 (1985).
7. K. L. F. Bane, "Landau Damping in the SLC Linac," SLAC-PUB-3670 (1985); Proc. Accelerator Conf., Vancouver B.C., Canada, May 13-16, 1985.
8. R. Ruth, "Emittance Preservation," to be published.
9. In Ref. 6, the dependence is given as  $W \propto \alpha^{-1.7} \lambda^{-3}$ . However, from theoretical considerations there should be no  $\lambda$  dependence for sufficiently short bunches. See SLAC Internal Report AAS-23 (1986).
10. K. Brown, private communication.
11. P. B. Wilson, "Future  $e^+e^-$  Linear Colliders and Beam-Beam Effects," SLAC-PUB-3985 (1986); Proc. Stanford Linear Accelerator Conference, June 2-6, 1986. [Note that in this paper an enhancement of the beamstrahlung is included incorrectly in the flat beam case.]
12. R. Hollebeek and A. Minten, SLAC Internal Report CN-302 (1985).
13. A. Minten, SLAC Internal Report, CN-305 (1985), and K. Yokoya SLAC Internal Report AAS-27 (1987); P. Chen and K. Yokoya, "Maximum Disruption Angles from Beam-Beam Interactions in Linear Colliders," SLAC-PUB-4339, 1987 (to be published).
14. R. J. Noble, SLAC-PUB-3871 (1986).
15. P. Wilson, "Linear Accelerators for TeV Colliders," Laser Acceleration of Particles, AIP Conf. Proc. #130, p. 560. See also SLAC-AAS-Note #2.
16. G. E. Fischer, "Ground Motion and Its Effects in Accelerator Design," SLAC-PUB-3392 Rev. and Proc. Particle Accelerator Conf., Batavia, Illinois, Aug 1984.
17. Alex Chou, reported at this Workshop.
18. R. B. Palmer, SLAC-PUB-3688.
19. Wolfgang Schnell, reported at this Workshop.

## APPENDIX I. Parameters Independent of Wavelength

Center-of-mass energy	$E = 1.0$ (TeV)
Maximum accelerating gradient	$\mathcal{E}_a = 186$ MeV/M
Overall length (excluding final focus)	$\ell = 6.8$ km
Bunch length/wavelength	$\sigma_x/\lambda = 1.5 \times 10^{-3}$
Final spot width/height	$R = 180$
Vertical disruption enhancement	$H_D = 2.37$
Crossing angle/maximum disruption angle	$\theta_c/\theta_D = 12$
Final focus quadrupole pole tip fields	$B_q = 1.4$ Tesla
Momentum spread at final focus	$\sigma_p(\text{focus}) = .15\%$
$\sigma_p(\text{from long emittance})/\sigma_p(\text{from wakefields})$	$F\sigma_p = .7$
$\beta^*$ (horizontal)/ $\beta^*$ (vertical)	$\beta_x^*/\beta_y^* = 324$
Vertical $\beta^*$ reduction from chromatic correction	27
Horizontal $\beta^*$ reduction from chromatic correction	.5
<b>Linac</b>	
Linac quad pole tip fields,	$B_{\ell q} = 1.4$ (Tesla)
Quad fraction of length	$F_{\ell q} = 5\%$
Linac quad aperture/linac iris aperture	$R_{qa} = 1.26$
Phase advance per cell	$\phi_{\ell} = 90^\circ$
Momentum spread for Landau damping	$\sigma_p(\text{Landau}) = .8 \times 10^{-3}$
Phase advance to maintain $\sigma_p(\text{Landau})$	$\phi = 27^\circ$
Length at end to correct $\sigma_p(\text{Landau})$	$\ell_c = 210$ m
Linear momentum spread from wakes	$1\sigma_p = .58\%$
Second order momentum spread from wakes	$2\sigma_p = .01\%$
Third order momentum spread from wakes	$3\sigma_p = .12\%$
Second order momentum spread from acceleration	negligible
<b>RF System</b>	
RF Structure group velocity	$v_g/c = \beta_g = .08$
Peak RF field/acceleration gradient	$\mathcal{E}_{pk}/\mathcal{E}_a = 2.6$
Normalized elastance	$s_{at} = 2.1 \times 10^{10}$ VmC <sup>-1</sup>
Fill time/attenuation time	$\tau = .25$
Fill efficiency	$\eta_p = .78$
RF structure loading	$\eta = 1.2\%$
RF source efficiency	$\epsilon_{RF} = 36\%$
Wall power consumption,	$W_{\text{wall}} = 100$ MW
<b>Damping Ring</b>	
Damping ring longitudinal impedance,	$Z_{\ell}/n = .5 \Omega$
Damping ring ratio of emitances	$\epsilon_x/\epsilon_y = 100$
Bending fields	$B_d = 2$ Tesla
Damping ring focus peak fields	$B_q = 1.4$ Tesla
Aperture	$a_{dr} = 12$ mm
Beta ratio: vertical/horizontal	$\beta_x/\beta_y = 4$
Partition functions	$J_x, J_y, J_z = 1, 1, 2$

**APPENDIX II. Parameters Dependent of Wavelength**

Criterion		Wavelength (mm)			
		35	26	17	12
Max Luminosity $10^{33} \text{ cm}^{-2} \text{ sec}^{-1}$	$\mathcal{L}_{\text{max}}$	1.7	1.7	1.3	1.0
Beamstrahlung $E$ loss	$\delta$	(.5)	.33	.17	.10
Beamstrahlung quantum parameter	$\Upsilon$	2.0	1.8	1.5	1.2
Frequency	Hz	55	100	220	500
Final spot size (vertical) (nm)	$\sigma_y$	1.5	1.3	1.0	.8
Final spot size (horizontal) ( $\mu\text{m}$ )	$\sigma_x$	.27	.23	.19	.15
Particles per bunch ( $10^{10}$ )	$N$	3.2	1.8	.8	.35
Bunch length (mm)	$\sigma_z$	.053	.04	.026	.018
Vertical Disruption	$D_y$	(24)	14	6	3
<b>Final Focus</b>					
Final focus (vertical) $\beta^*$ (mm)	$\beta_y^*$	.051	.047	.043	.038
Final focus (horizontal) $\beta^*$ (mm)	$\beta_x^*$	17	15	14	12
Maximum horizontal disruption angle (mrad)	$\theta_{xD}$	24	14	6	3
Final convergent angle (horizontal) (mrad)	$\theta_{fz}$	.016	.015	.014	.012
Final convergent angle (vertical) (mrad)	$\theta_{fy}$	.030	.027	.025	.022
Bunch diagonal angle (mrad)	$\theta_{\text{diag}}$	5.1	5.8	7.3	8.3
Crossing angle (mrad)	$\theta_c$	(6)	4	2.2	1.2
First quad aperture (mm)	$a_q$	.15	.13	.10	.08
Length to first quad (m)	$l^*$	.47	.43	.39	.35
Length to sweep quantum disruption (m)	$l_s$	(.84)	(.56)	.30	.17
<b>Wakes</b>					
Transverse wake potential V $\text{pC}^{-1} \text{ m}^{-2}$	$W_t(2\sigma_x)$	1.5k	3.7k	12k	43k
Average $\beta$ in linac (m)	$\beta_{\text{linac}}$	19	17	14	11
Delta phase advance (radians)	$\Delta\phi$	.16	.18	.22	.27
Number of quads in linac	$N_q$	340	390	480	580
Vertical alignment tolerance ( $\mu\text{m}$ )	$\langle\Delta y\rangle$	122	93	66	44
Longitudinal wake (at $z = 0$ ) V $\text{pC}^{-1} \text{ m}^{-2}$	$W_l(0)$	580	1k	2.3k	5.2k
<b>Damping Ring</b>					
Normalized emittance (vertical) $10^{-8} \text{ m}$	$\epsilon_{ny}$	4.4	3.5	2.5	1.8
Normalized emittance (horizontal) $10^{-6} \text{ m}$	$\epsilon_{nz}$	4.4	3.5	2.5	1.8
Longitudinal emittance m	$\epsilon_x$	.044	.033	.022	.015
Energy (GeV)	$E_{dr}$	0.98	1.0	1.04	1.09
Ring radius (m)	$R$	12.3	14.6	18.2	23.3
Tune (horizontal)	$Q_y$	17.7	20.7	25.3	31.8
Tune (vertical)	$Q_x$	4.4	5.2	6.3	7.9
bunch length (cm)	$\sigma_z$	(3.4)	(2.4)	1.5	1.0
momentum spread ( $10^{-3}$ )	$\sigma_p$	.68	.69	.70	.72
$E$ loss Volts/turn (MV)	$U$	.17	.22	.29	.40
Damping time constant (msec)	$\tau$	2.35	2.28	2.20	2.11
Impedance requirement ( $\Omega$ )	$Z$	(183)	300	600	1200

APPENDIX II, continued

Criterion	Wavelength (mm)				
	35	26	17	12	
<u>RF System</u>					
Wavelength (mm)	$\lambda$	35	26	17	12
Elastance $V \text{ pC}^{-1} \text{ m}^{-2}$	$S_i$	440	800	1760	3960
$Q$	$Q$	8.3k	7.2k	5.8k	4.8k
Iris radius (mm)	$a$	6.93	5.2	3.46	2.31
Inside cavity radius (mm)	$b$	14.9	11.2	7.4	5.0
RF pulse length (nsec)	$t$	71	45	25	(14)
Length per feed (m)	$L$	1.8	1.2	.65	.35
Peak power per m (GW)	$W_{pk}/\ell$	1.4	1.2	1.0	.82
Total peak power (TW)	$W_{pk}$	.92	.80	.66	.53
Total RF energy (kJ)	$J$	(652)	(367)	164	72

Parenthesised values have some difficulty or objection.